Impact of high shear blending on distribution of magnesium stearate on lactose for dry powder inhaled formulations

Alexander Welle [a,*], Mohit Mehta [b], Karin Marek [b], Harry Peters [c], Peter van der Wel [d], Olukayode Imole [d]

[a] Karlsruhe Nano Micro Facility, Institute for Functional Interfaces, Karlsruhe Institute of Technology, Hermann-von-Helmholtz-Platz 1, 76344 Eggenstein-Leopoldshafen, Germany
[b] Harro Höfliger Verpackungsmaschinen GmbH, Helmholtzstraße 4, 71573 Allmersbach i.T., Germany
[c] DFE Pharma GmbH, Kleverstrasse 187, 47568 Goch, Germany
[d] Hosokawa Micron B.V., Gildenstraat 26, 7005 BL, Doetinchem, the Netherlands

ARTICLE INFO

Keywords:
Dry Powder Inhaler
Lactose
Magnesium Stearate
Time-of-Flight Secondary Ion Mass Spectrometry
Powder Flow

ABSTRACT

The use of magnesium stearate along with lactose in Dry Powder Inhaler (DPI) formulations is increasing.

The impact of different conditions of high shear blending on the distribution of magnesium stearate on lactose particles was investigated in this study. The formulated blends were manufactured using high shear blending of pre-blended coarse and fine lactose particles with 1.0% (w/w) magnesium stearate under different blending conditions, specifically blending speed and time. The effects of blending conditions on the distribution of magnesium stearate on lactose particles were clearly identifiable by characterizing the formulated blends by means of rheological evaluations, scanning electron microscopy, and chemical surface analysis using time-of-flight secondary ion mass spectrometry (ToF-SIMS). Rheological properties were significantly affected in blends with magnesium stearate compared to blends without magnesium stearate. Blending speed exhibited a strong influence on the distribution of magnesium stearate on lactose surface, while blending time had relatively minor effect.

1. Introduction

The history of dry powder inhalers (DPIs) spans more than 100 years. However, the first commercial product, Abbott's "Aerohaler", for the delivery of penicillin and norethisterone was launched in 1948. It was a capsule-based device that served as model for next generations of DPIs to come (de Boer et al., 2017). Most DPI formulations are targeted to treat asthma and Chronic Obstructive Pulmonary Disease (COPD) based on highly potent drugs requiring significantly low doses. To achieve significant deposition into the lungs, the active pharmaceutical ingredients (APIs) need to be micronized. This approach, however, would lead to poor flowability of the APIs. Therefore, DPIs are manufactured as carrier-based systems using lactose as a carrier excipient. The addition of lactose serves to increase the volume of the formulation and to improve flow of the formulation, facilitating filling into capsules or blisters. Lactose can also improve aerosolization of the formulation leading to significant deposition in the lungs (Kinnunen et al., 2015).

Several studies focused on understanding the impact of lactose fines on *in-vitro* lung deposition have been reported in literature. Kinnunen et al. demonstrated that inclusion of lactose fines resulted in a significant increase of the fine particle fraction deposition of Budesonide DPI formulations into the lungs (Kinnunen et al., 2014). However, they also observed that if the amount of lactose fines is increased significantly, it could lead to a negative impact on fine particle fraction deposition due to increased cohesivity and reduced dispersion forces. Hertel et al. focused on understanding the optimal concentration of lactose fines required for DPI formulations using Salbutamol sulphate as model drug (Hertel et al., 2018). The authors demonstrated a good correlation between the powder flow properties and fine particle fractions. Furthermore, it was observed that the addition of extreme high concentrations of lactose fines into the formulation can lead to the formation of agglomerates between fine lactose and API particles. This could lead to a drop in the fine particle fraction and eventually a reduction in aerodynamic performance. Sun et al. conducted similar studies using Salbutamol sulphate as a model drug and demonstrated that lactose fines between 0 and 11 μm showed good correlation to fine particle fraction of

* Corresponding author.
E-mail address: alexander.welle@kit.edu (A. Welle).

the formulations (Sun et al., 2022). Particles exceeding 11 μm in size would act as a second carrier, which increases the drug adhesion to these lactose particles.

There has been a noticeable shift from the use of single excipient formulations to dual excipients in newly developed DPI formulations (Shur et al., 2016). These formulations comprise of magnesium stearate as an excipient along with lactose as carrier. Magnesium stearate is used for variety of reasons such as to improve stability of the API, as flow enhancer or to enhance the deposition of the API in DPI formulations. Several studies have investigated the influence of magnesium stearate on the rheological and aerodynamic performance of formulations. R. Guchardi and coworkers demonstrated an impact of magnesium stearate on aerodynamic performance of Formoterol fumarate dihydrate (Guchardi et al., 2008). They concluded that by adding magnesium stearate to lactose-based formulations, the interaction between fine and coarse lactose particles increases. This reduces active free sites which enhances the delivery efficacy of the Formoterol fumarate. Jetzer et al. investigated the impact of magnesium stearate addition to lactose-based dry powder inhaled (DPI) formulations focusing on different blending techniques, highlighting the importance of high shear blending (Jetzer et al., 2018). It has also been demonstrated that magnesium stearate can act as a barrier inhibiting or reducing chemical interactions between lactose and the API, especially if the API is prone to degradation due to interactions with lactose (Monteith et al., 2004). To serve as a substantial barrier, a uniform coating of magnesium stearate on the carrier particles is essential. In case of tablet formulations, the magnesium stearate is used to reduce stickiness during the tableting process. In such cases, magnesium stearate is blended for a short duration to avoid dissolution-related issues (Bolhuis et al., 1987). However, based on its role in DPI formulation as substantial barrier, a more intensive blending may be required. This can typically be achieved through high shear blending (Hebbink et al., 2022) or mechano-chemical bonding using high shear compressive forces (Green et al., 2009).

Although the impact of magnesium stearate coatings applied on lactose particles using high shear blending is very well studied and demonstrated (Jetzer et al., 2018), the authors consider it important to further investigate the effect of blending speed and time on the magnesium stearate coating on lactose particles.

Secondary Ion Mass Spectrometry (SIMS) but also X-Ray Photoelectron Spectroscopy (XPS) have been previously applied to study not only properties of tablets obtained by wet granulation or direct compression (Mitchell et al., 2006), but also in particle studies for inhalation applications (Jetzer et al., 2018; Qu et al., 2015; Zhou et al., 2011). Both analytical methods share a low probing depth. However, due to the molecular characterization, SIMS provides an unambiguous assignment of core and shell species like lactose and magnesium stearate. When performed in quasi-static mode using limited primary ion fluences, SIMS is non-destructive and provides mass spectra with parallel detection of elements like magnesium and larger organic fragments and adducts. For an overview of other analytical techniques applied in studies of DPI formulations the reader is referred to (Weiss et al., 2015).

The objective of this study is to investigate effects of blending speed and time on the particle size distribution and flow properties of the blends. Further, the investigation is also carried out to characterize the extent of surface coating of lactose with magnesium stearate based on ToF-SIMS data.

2. Materials and methods

2.1. Material characteristics

Two different standard Lactohale® products (LH206 and LH230) were sourced from DFE Pharma (Borculo, The Netherlands). LH206 is milled lactose with tightly controlled particle size devoid of any fine particles and serves as a carrier. Whereas, LH230 is finely milled lactose with irregular shaped particles and is typically employed to enhance the cohesiveness of the powder blends and promote drug deposition into the lungs (Kinnunen et al., 2014). In addition, magnesium stearate (LIGAMED MF-2-V PREMIUM), sourced from Peter Greven GmbH & Co. KG (Bad Münstereifel, Germany) was used. The particle size distributions and bulk densities of the excipients are presented in Table 1.

2.2. Lactose pre-blends

The lactose pre-blend (6.0 kg) was prepared using a low shear 10-liter Nauta conical screw blender (Hosokawa Micron B.V.), shown in Fig. 1(a). LH206 (coarse lactose) and LH230 (fine lactose) were pre-blended in a ratio of 80:20 (w/w) at a blending screw speed of 150 rpm for 15 mins.

2.3. Magnesium stearate blending with preblended lactose

Magnesium stearate 1.0 % (w/w) was blended with the pre-blended lactose using a 1-liter Cyclomix high shear blender (Hosokawa Micron B. V) (see Fig. 1(b) (Rahmanian et al. (2008)). The batch size for each experiment was 700 g. First, half of the total batch size was charged into the blender, followed by the addition of magnesium stearate. Thereafter, the second half of the lactose pre-blend was added on top, such that the magnesium stearate was sandwiched between the lactose pre-blends.

High shear blenders are used when blending ordered mixtures with APIs, or when coating with magnesium stearate is required. In the Cyclomix high shear blender (Fig. 1 (b)), the centrifugal force from the rotating paddles pushes the particles towards the wall of the vessel. The shear required for coating is introduced in the clearance between the rotor paddles and the wall. The particles are transported upwards along the wall to the free space beneath the upper dome, fall through the centre of the blender, and are recirculated in a vortex-like pattern (see Fig. 1(b)) (Rahmanian et al. (2008)). The shear at the wall leads to an increase in the product temperature. To maintain the temperature within acceptable limits, a cooling jacket is used to control the temperature of the product.

Two sets of experiments were performed. The first set focused on investigating the impact of blending speed on the coating of magnesium stearate on pre-blended lactose. These experiments were conducted at different blending speeds as listed in Table 2. Temperature for all blending experiments was controlled between 20 and 22 °C by circulating cold water through the jacket of the blender. The blends produced were analysed for particle size distribution (PSD), flow properties, coating efficiency and morphological characteristics.

The optimal blending speed resulting in blends with favourable flow properties and coating efficiency, served as the initial value for the second set of experiments to investigate the impact of blending time on the coating of magnesium stearate on preblended lactose. These experiments were conducted at different blending times, maintaining a constant blending speed, see Table 2. The obtained blends were subsequently analysed for their PSD, flow properties, coating efficiency and morphological characteristics.

As a comparison, blending speeds in a Nauta blender typically range between 0.1 and 2 m/s, whereas in a Cyclomix blender they can vary from 5 to 25 m/s. The overall power required depends on various factors, but as rule of thumb, in a Nauta blender 10 W/kg is required for mixing while in a Cyclomix blender 1000 W/kg is applied.

Table 1
Particle size distributions and density of the excipients.

Property		Unit	LH206	LH230	Magnesium Stearate
Size distribution	X_{10}	μm	33	1.4	1.2
	X_{50}	μm	83	8.4	4.9
	X_{90}	μm	154	23	22.3
Bulk density		g/l	720	310	240

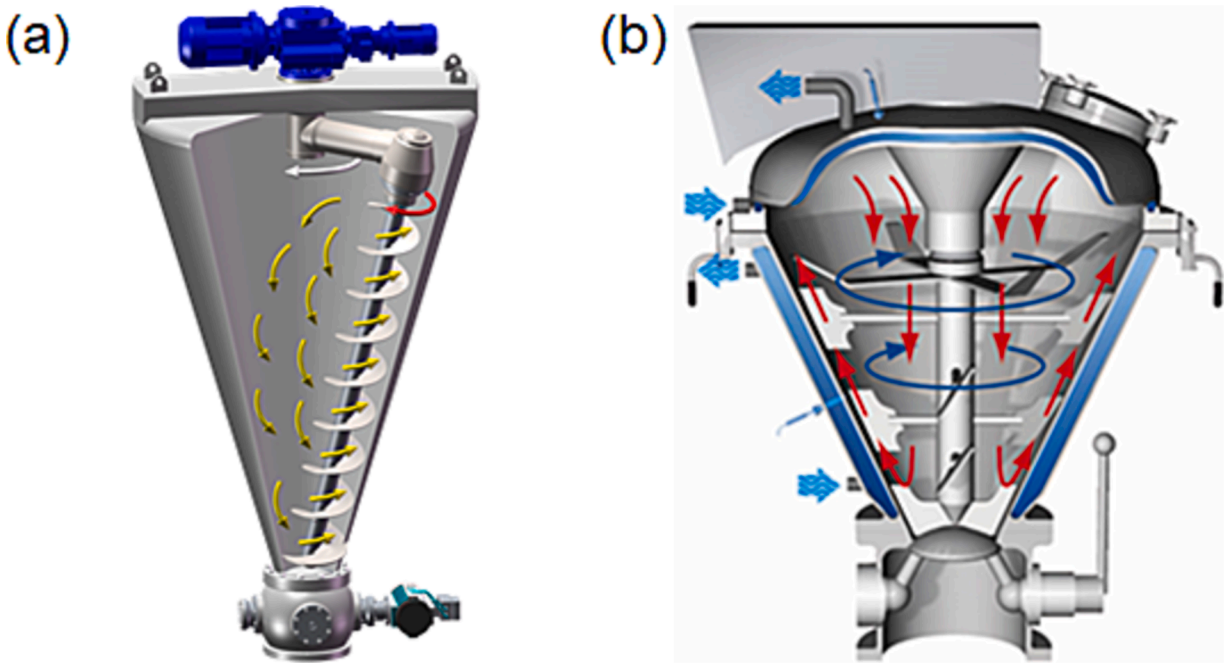

Fig. 1. Schematic representation of (a) the Nauta blender used to prepare the lactose pre-blends (left), and (b) the Cyclomix high shear blender for blending the different lactose grades with magnesium stearate (right).

Table 2
Process settings used in the experiments.

Experiment	Batch name	Blending speed (rpm)	Tip speed (m/s)	Blending time (minutes)
Set - I	CLX1	500	3.3	10
	CLX2	1000	6.6	10
	CLX3	1500	9.9	10
	CLX4	2000	13.2	10
	CLX5	2500	16.5	10
Set - II	CLX-T1	1500	9.9	5
	CLX-T2	1500	9.9	10
	CLX-T3	1500	9.9	15

2.4. Characterization techniques

2.4.1. Particle size distribution

The particle size distributions (PSD) of the powders were measured using a laser diffraction system (Sympatec GmbH, Clausthal-Zellerfeld, Germany) with an RODOS dry powder dispersing system and an Aspiros powder feeder (Sympatec GmbH, Germany) at a dispersing pressure of 1.5 bar. For all the blends the R4 lens was used. In addition to x10, x50 and x90 in the analysis of the PSD, the Q4.5 (particle fraction below 4.5 μm) was also considered.

2.4.2. Flow properties

All powders were analysed for bulk (ρ_B) and tapped densities (ρ_T) according to the USP method (United States Pharmacopeia, 2013) and Carr's index C (%) was calculated as below:

$$C[\%] = 100\frac{\rho_T \quad \rho_B}{\rho_T}$$

Powder flow properties for all powders were characterized using a FT4 powder rheometer (Freeman Technology, Welland, UK). Experiments were focused on measuring compressibility and flow factor.

2.4.3. Particle morphology – Scanning electron microscopy

The powders were analysed by scanning electron microscopy (SEM, G6 Phenom Pro; Thermo Fisher Scientific, Eindhoven, the Netherlands). The samples were mounted on aluminium SEM stubs with adhesive carbon tabs (Microtonano, Haarlem, Netherlands) and subsequently gold coated (6 nm) with a LUXOR Gold Coater (IB-FT GmbH, Berlin, Germany) in order to stabilize them and increase their electrical conductivity. Samples were analysed at a high voltage of 10 kV and a sample pressure of 1.0 Pa.

2.4.4. Water contact angle

Water contact angle measurements were conducted for all blends. Powders were loaded into a glass cylinder with a planar rim. Overfilling, followed by gently tapping the filled cylinder to allow the powder to settle and finally stripping the excess powder above the rim of the cylinder with a glass slide, yielded a flat, homogeneous powder bed. A small droplet of distilled water (approx. 10 μL) was then applied onto the powder using a syringe and needle without touching the powder bed (sessile drop). Using a Keyence Digital microscope VHX-2000 and the corresponding VHX software 2.3.1.9 (Keyence Deutschland GmbH, Neu-Isenburg, Germany) side-on images of several drops are taken and the water contact angles (WCA) are determined from the height, h, and the base width, b, of the droplet, according to (Cocconi et al., 2012) by:

$$WCA = \tan^{-1}\frac{2h}{b} \times 2 \times \frac{180}{\pi}$$

2.4.5. Time-of-Flight Secondary Ion Mass Spectrometry

Time-of-Flight Secondary Ion Mass Spectrometry (ToF-SIMS) was performed on a TOF.SIMS5 instrument (ION-TOF GmbH, Münster, Germany). A 25 keV Bi_3^+ cluster primary ion beam was applied, providing bunched ion pulses with a beam diameter of approx. 4 μm, a target current of 0.36—0.38 pA at 10 kHz repetition rate and 1.1 ns pulse length. The ultra-high vacuum base pressure during analysis was $< 3.5 \times 10^{-8}$ mbar. Samples were mounted by carefully dusting the powders onto conductive (graphite) sticky tape discs (Product No. G3347, Plano GmbH, Wetzlar, Germany) and removing excess powder by an argon flow. Additional charge compensation was achieved by applying a 21 eV electron flood gun and tuning the reflectron accordingly. Positive polarity secondary ion spectra / images were recorded from several spots, 500 × 500 μm^2 field of view, 128 × 128 data points,

on each specimen, data acquisition was stopped at the quasi static limit (2×10^{11} ions/cm^2). Mass scale calibration was based on low molecular weight hydrocarbon signals (CH_2^+, CH_3^+) and the $^{24}Mg^+$ and $^{26}Mg^+$ signals.

3. Results and Discussions

3.1. Blending of lactose preblends and magnesium stearate

Fine lactose particles are typically added to dry powder inhalation formulations, due to their significant influence on enhancing the aerodynamic performance of these formulations. However, an excessive presence of fine lactose particle can lead to negative effects due to agglomerations which may reduce the performance of the powder formulations (Mehta et al., 2018). Hence, a fine balance is required with more control over the lactose fines. Typically, dry powder formulations are processed using either a low shear blending or a high shear blending mechanism. Previous studies have shown that high shear blending can lead to *in-situ* generation of lactose fines due to high shear forces (Shur et al., 2008). This can significantly impact the quality of the powder formulations.

To avoid or to minimize the generation of additional fines during the lactose blending process, coarse and fine grade of lactose were blended using a low shear Nauta blender (see Fig. 1(a)). In the second blending step of mixing preblended lactose with magnesium stearate, the objective was to achieve significant coating of magnesium stearate on the lactose surface. In a previously published paper, Jetzer et al. studied the impact of low and high shear blending on the coating of magnesium stearate onto the lactose surfaces (Jetzer et al., 2018). There was significant coating observed with high shear blending as compared to low shear blending. In case of low shear blending, magnesium stearate agglomerates were detected by ToF-SIMS imaging as small intense spots, indicating inadequate surface coating of the lactose with the magnesium stearate. Therefore, it was concluded that high energy is required to yield an efficient coating of magnesium stearate on lactose. This energy or shear is required to break up the cohesive forces between the magnesium stearate particles and create a homogenous surface distribution of the stearate on the lactose particles.

3.2. Impact of blending speed and time on particle size distribution

Table 3 presents the results of the particle size and flow properties for the different blends. An increase in percentage fines in the blend (particles below 4.5 μm) was observed with the addition of magnesium stearate compared to plain preblends (LH206 + 20 % LH230). This increase could be attributed to the addition of the fine magnesium stearate particles having an X50 value of around 5 μm. However, with an increase in blending speed from 500 rpm (CLX1) to 1000 rpm (CLX2) a decrease in percentage fines (particles below 4.5 μm) was observed. This could be due to adhesion of the magnesium stearate particles onto the surface of the lactose particles, leading to a reduced percentage of fine individual magnesium stearate particles in the blend. A further increase in the blending speed to 1500 rpm – 2000 rpm (CLX3 and CLX4), showed only a marginal increase in percentage fines. However, with further increase in the blending speed to 2500 rpm (CLX5), a significant increase in percentage fines was observed. This observation shows good correlation with SEM images. Initially, this effect is relatively low, Fig. 2 (a) to (e), however, the run CLX5 with increased speed yields a larger number of fine particles adhering to the coarser lactose is observed (Fig. 2 (f)). This could be attributed to a chipping of coarser lactose particles into fines leading to an increase of fine particles. Based on the PSD data, it was determined that 1500 rpm (CLX3) represented the optimal blending speed, where the values for Q4.5 μm (percentage fines in the blend / particles below 4.5 μm) appeared to stabilize, with minimal generation of new fines, see Table 3. (Fig. 3.).

Blending time experiments were conducted at a constant blending speed of 1500 rpm (CLX3 – optimal speed). No significant differences were observed in PSD values with different blending time of 5, 10 or 15 min. This implies that blending time has a negligible impact at the given blending speed. However, the impact of blending time at other blending speeds needs further investigation.

3.3. Impact of blending speed and time on blend flow properties and extent of coating

The addition and blending of magnesium stearate with lactose resulted in an increase in both bulk and tapped densities of the powders, with a more pronounced impact on the tapped densities. Therefore, the Carr's index decreased for all the powders. The decrease in Carr's index stabilized once a blending speed of 1000 rpm was achieved. The change in compressibility followed the same pattern as the Carr's index. Regarding the flow factor data, the addition of magnesium stearate led to an increase in flow factor values. The changes observed in Carr's index, compressibility and the flow factor indicate an increase in flowability of the powders after blending with magnesium stearate. These changes could be attributed to the distribution of magnesium stearate on the surface of the lactose particles, leading to a lower cohesivity between the particles.

The wettability of the blends determined from water contact angle (WCA) measurements shows obvious changes. The measurement of contact angles on powder samples is more complex than analysing shapes of droplets on flat, solid and homogeneous surfaces. Based on the water solubility of lactose, further difficulties arise, e.g. making capillary rise experiments impossible. These difficulties are described in literature (Alghunaim et al., 2016; Chander et al., 2007; Depalo and Santomaso, 2013; Galet et al., 2010b; Teipel and Mikonsaari, 2004;

Table 3
Particle size distribution and flow and wetting properties of Lactose / Mg stearate blends for different blending speed and time.

Test Method	Unit	Preblend LH206 + 20 % LH230	CLX1	CLX2	CLX3	CLX4	CLX5	CLX-T1	CLX-T2	CLX-T3
Blending speed	rpm	–	500	1000	1500	2000	2500	1500	1500	1500
Blending time	min	–	10	10	10	10	10	5	10	15
Carr's Index	%	38	34	26	30	30	34	28	28	28
Bulk density	g/ml	0.58	0.66	0.83	0.78	0.79	0.83	0.83	0.82	0.83
Tapped density	g/ml	0.93	1.01	1.12	1.11	1.13	1.15	1.16	1.14	1.16
Particle size distribution										
x10	μm	3.3	2.9	3.0	2.7	2.6	2.1	2.9	2.8	3.2
x50	μm	52.1	50.4	57.8	55.9	58.1	59.0	55.7	54.7	57.3
x90	μm	122.6	120.3	125.0	121.1	123.0	124.8	121.3	120.8	122.4
Q4.5 μm	%	12.9	14.5	13.4	14.4	14.7	17.3	13.9	14.1	13.0
Flow characteristics										
Compressibility @15 kPa	%	25.1	20.9	8.3	11.7	12.2	13.7	10.8	9.8	10.9
Flow Factor	–	4.2	6.8	6.8	8.4	5.2	5.4	5.1	5.1	6.0
Wettability										
Water Contact Angle	°	0	0	107	111	114	114	114	113	111

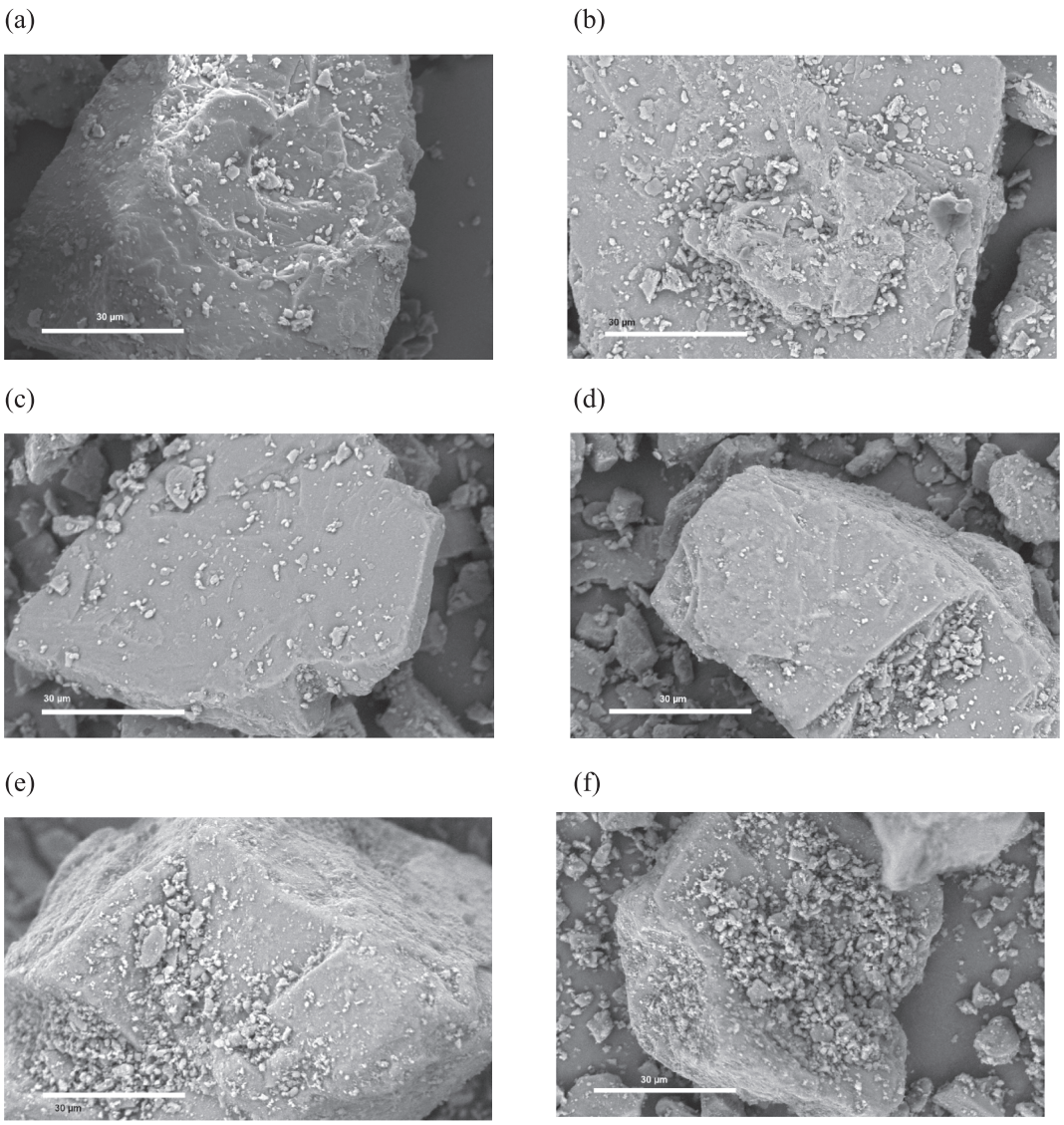

Fig. 2. Scanning electron micrographs of (a) the pure lactose mixture, and (b-f) different lactose / magnesium stearate blends (see Table 2). (b) CLX1 / 500 rpm; (c) CLX2 / 1000 rpm; (d) CLX3 / 1500 rpm; (e) CLX4 / 2000 rpm; and (f) CLX5 / 2500 rpm. All scale bars 30 µm.

Wang et al., 2023) and necessitated the development of new analytical methods like the Broadband Acoustic Resonance Dissolution Spectroscopy (Peddapatla et al., 2018). Despite these methodological problems, water contact angles of the blends, measured in a reproducible setup, can provide additional insights into the stearate coating of lactose. As shown in Table 3, the pure lactose preblend and the powder obtained by blending at 500 rpm only (CLX1) are very hydrophilic and fully wettable by water. For the blend obtained with 1000 rpm blending speed (CLX2) the first evidence of the hydrophobization of the lactose by the magnesium stearate appears. With increasing blending speed, the WCA levels off around 113°. For pure magnesium stearate powder Galet et al. reported a WCA of 125° (Galet et al., 2010a). The water contact angle is not sensitive to the chipping of the lactose particles at very high blending speeds (CLX5). The fraction of fines increased at 2500 rpm blending speed, but obviously the hydrophilic lactose gets sufficiently covered by stearate again keeping the blend hydrophobic.

No significant impact was observed for different blending times concerning compressibility and flow factor. It was observed that CLX3 and CLX-T2 (blends with same conditions) which yielded reproducible results for PSD and compressibility, failed to show reproducibility in terms of the flow factor. This could be attributed to the inherent complexity and associated variability in the measurement of the flow factor with FT4 measurements.

3.4. Evaluation of impact of blending speed and time on magnesium stearate coating using ToF-SIMS

While in SIMS the signal for the stearate anion, $C_{18}H_{35}O_2^-$, is rather prominent for stearic acid, the intensity for Mg stearate is rather low. Consequently, this signal will not be used for coverage quantification. However, since pure lactose particles exhibit a very low magnesium background, the Mg^+ signal is indicative for magnesium stearate. For the detection of lactose, Jetzer et al. (Jetzer et al., 2018) proposed the use of three small fragments of lactose: CH_3O^+, $C_2H_5O^+$, and $C_3H_5O_2^+$. These fragments were used to quantify the coverage of magnesium stearate on lactose particles according to:

$I(Mg^+) / \Sigma (I(Mg^+), I(CH_3O^+))$, etc.

We have identified two more lactose-indicating signals in the high mass range of the spectra: Alkaline metal adducts of intact lactose molecules, $C_{12}H_{22}O_{11}Na$ at 365 *m/z*, and $C_{12}H_{22}O_{11}K$ at 381 *m/z*, referred as Lac-Na and Lac-K, respectively. Using these peaks instead of the smaller fragments CH_3O^+, $C_2H_5O^+$, and $C_3H_5O_2^+$, as applied by Jetzer et al. (Jetzer et al., 2018), provided robust data by eliminating potential interfering signals at lower masses. One example of a

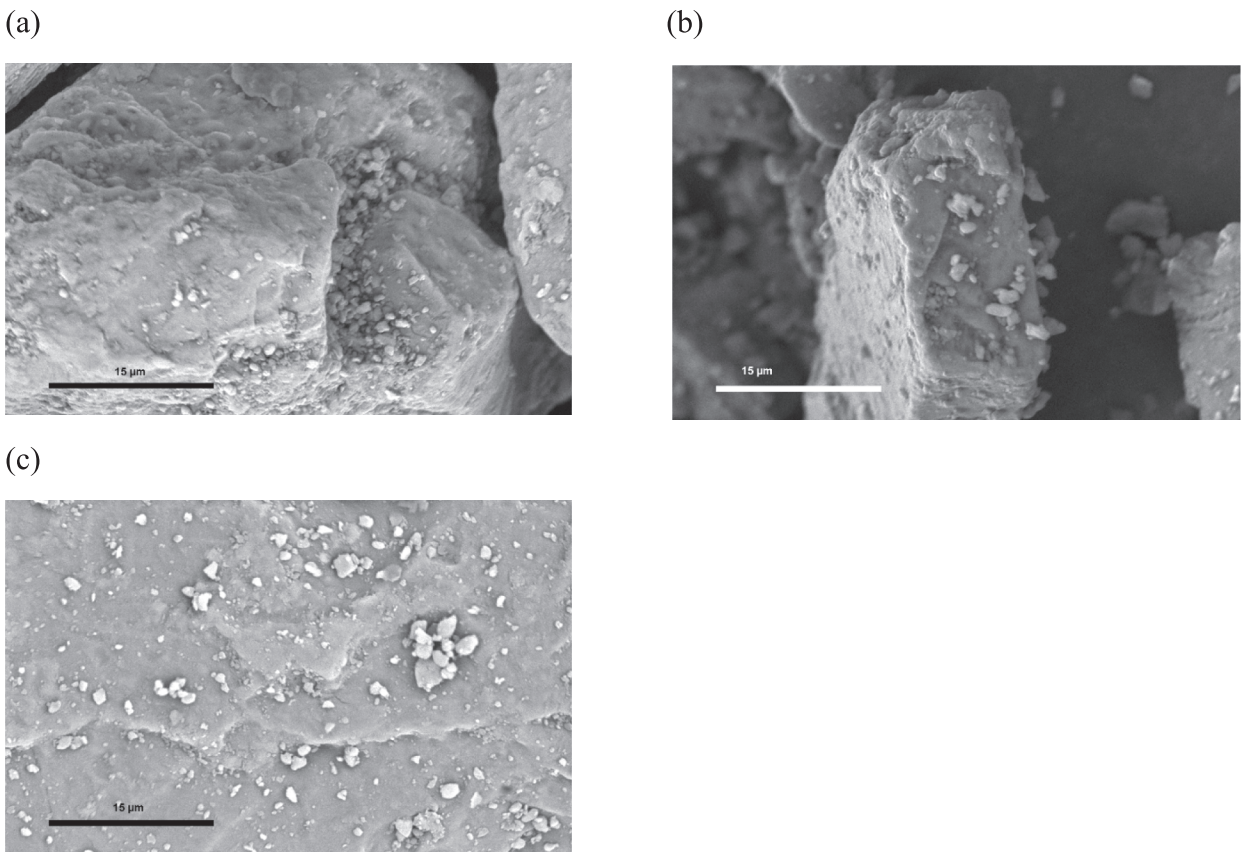

Fig. 3. Scanning electron micrographs of different blends from several blending times at constant blending speed 1500 rpm, (see Table 2). (a) CLX-T1 / 5 min; (b) CLX-T2 / 10 min, (c) CLX-T3 / 15 min. All scale bars 15 µm.

potentially interfering compound is $SiC_3H_9^+$, a prominent SIMS signal from silicone oils, at 73.0468 *m/z*, nearby to $C_3H_5O_2^+$ at 73.0284 *m/z*. While this is usually no problem for many SIMS analyses having usually a mass resolution in the range of > 6000 M/ΔM; the non-conductive powder samples presented a technical challenge due to peak shifts and broadening as seen in the raw data, inserts in Figs. 4-6. As shown, peak splitting and broadening were observed due to the roughness and uneven electrical potentials of the sample. To compensate these local

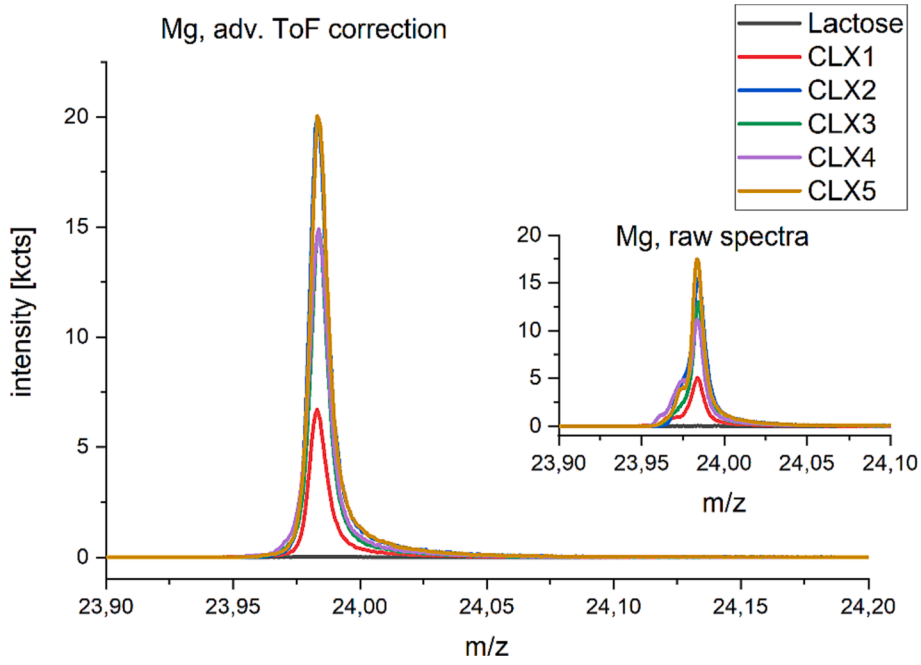

Fig. 4. SIMS signals of magnesium for pure lactose and different magnesium stearate / lactose blends, (see Table 2). Insert: Raw data. Main graph: Data with advanced ToF correction.

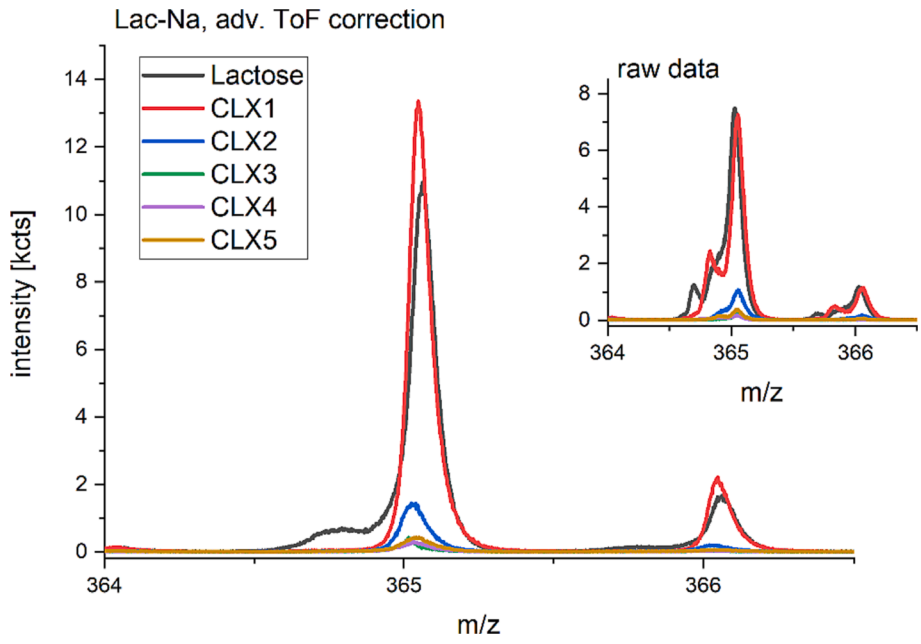

Fig. 5. SIMS signals of $C_{12}H_{22}O_{11}Na$, Lac-Na, for pure lactose and different magnesium stearate / lactose blends, (see Table 2). Insert: Raw data. Main graph: Data with advanced ToF correction. Note that for pure lactose (black lines) even corrected data show a slight tailing.

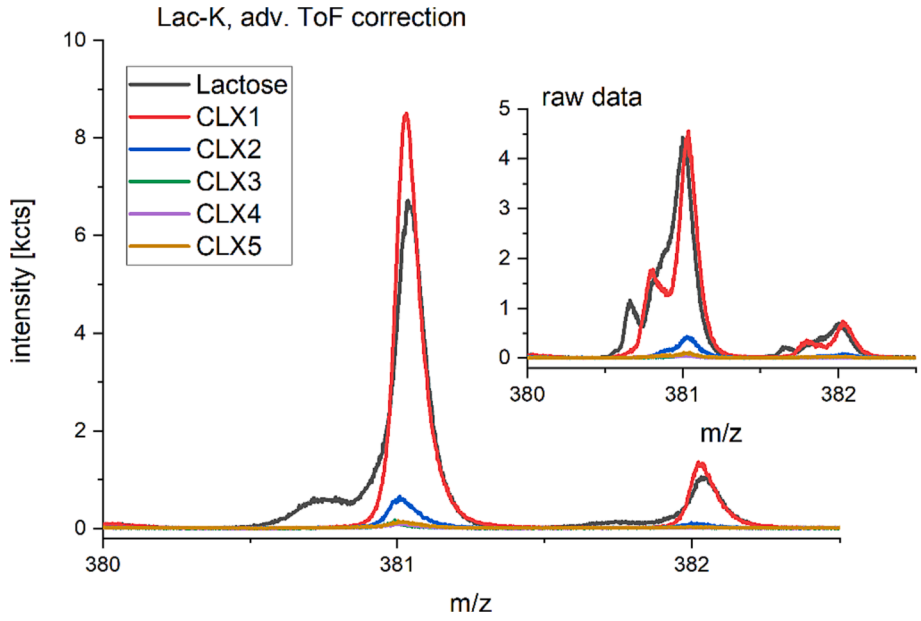

Fig. 6. SIMS signals of $C_{12}H_{22}O_{11}K$, Lac-K, for pure lactose and different magnesium stearate / lactose blends, (see Table 2). Insert: Raw data. Main graph: Data with advanced ToF correction. Note that for pure lactose even corrected data show a slight tailing.

effects spectra can be subjected to an advanced time-of-flight correction. Using this data analysis method, pixel-wise corrections are performed on the flight-time-to-mass conversion. The raw data shown are based on a single mass scale calibration of the total spectrum (all scans, all pixel). Corrected data typically yield improved mass resolution and peak shape by adjusting the mass scale individually for each pixel within the analyzed field of view (128 × 128 pixel from 500 × 500 μm^2 area).

In conclusion, the careful selection of robust and reliable marker peaks, such as Lac-Na and Lac-K offering high signal/noise ratios, a high dynamic range and the lowest risk of cross-talk with potential interfering signals, is crucial in the design of SIMS studies. In the following we will use the ratio I(Mg^+) / I(Lac-K^+), plotted in Fig. 7, to indirectly quantify the coverage of lactose particles with magnesium stearate. At blending speeds of 500 and 1000 rpm, a low ratio was obtained, indicating incomplete coverage of magnesium stearate on the lactose surface. As the blending speed increases to 1500 rpm (CLX3) and 2000 rpm (CLX4), a maximum ratio was achieved, suggesting maximal coverage of magnesium stearate on the lactose. However, a further increase to 2500 rpm (CLX5) resulted in a decrease of the ratio. In conjunction with the particle size data and the SEM pictures (Fig. 2) this decrease is attributed to a damage to the lactose particles, as evidenced by indicators for non-coated particle surfaces form the Lac-K SIMS signals.

Blending time did not exhibit any significant impact on particle size, contact angle or powder flow. However, in the ToF-SIMS data (Fig. 8) the 5 min blending time (CLX-T1) showed a lower magnesium/lactose ratio.

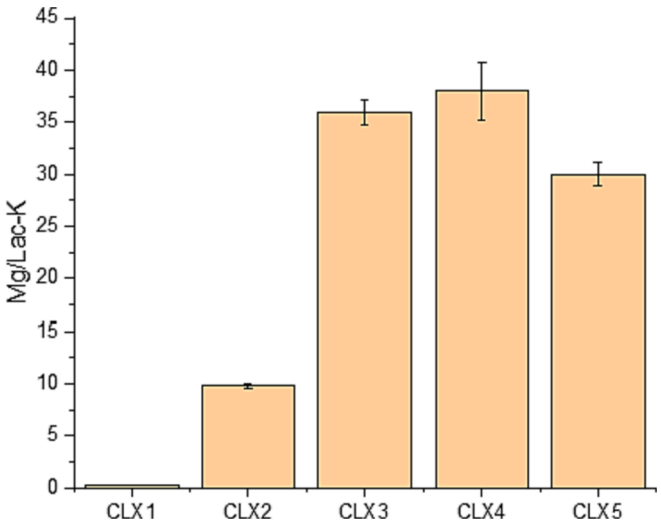

Fig. 7. SIMS signal ratio of Mg^+ / Lac-K^+ for a blending time of 10 min and blending speeds from 500 to 2500 rpm according to preparation protocol in Table 2.

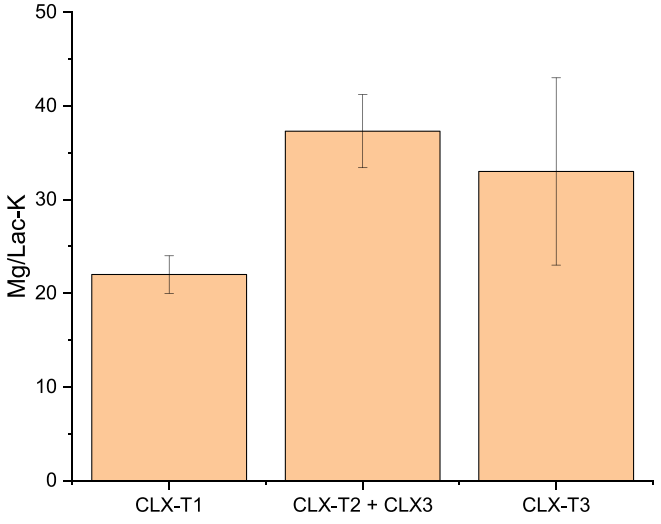

Fig. 8. SIMS signal ratio of Mg^+ / Lac-K^+ for 1500 rpm blending speed and increasing blending time of 5 min (T1, n 4), 10 min (T2 + CLX3, n 8), and 15 min (T3, n 4) respectively. See also Table 2.

While the calculated signal ratios based on the quantification according to Jetzer (Jetzer et al., 2018), shown in Table 4, approach unity for pure magnesium stearate, we have observed especially for the $C_3H_5O_2^+$-signal derived ratio a clear discrepancy and a rather high level of experimental error in our data.

Having established that 1500 rpm (CLX3) represents the lowest blending speed resulting in coverage saturation, as determined by SIMS, we proceeded to investigate the effects of blending time. As shown above in Fig. 8, the 5 min blending time performed in run T1 yielded a lower magnesium stearate coverage as compared to T2 with 10 min of blending. Increasing blending time further to 15 mins did not result in a further increase in coverage, as shown in Fig. 8, and Table 5 for the alternative calculation according to (Jetzer et al., 2018).

Table 4
SIMS signal ratios for I(Mg^+) / Σ (I(Mg^+), I(CH_3O^+)), I(Mg^+) / Σ (I(Mg^+), I($C_2H_5O^+$)), and I(Mg^+) / Σ (I(Mg^+), I($C_3H_5O_2^+$)), respectively.

	CH_3O^+ basis	$C_2H_5O^+$ basis	$C_3H_5O_2^+$ basis
Lactose (n = 3)	0.003 ± 6.6 × 10^{-4}	0.002 ± 4 × 10^{-4}	7 × 10^{-4} ± 1 × 10^{-4}
Mg stearate (n = 3)	0.98 ± 0.01	0.96 ± 0.03	0.7 ± 0.2
CLX1 (n = 4)	0.24 ± 0.01	0.20 ± 0.01	0.08 ± 0.01
ClX2 (n = 4)	0.82 ± 0.01	0.78 ± 0.01	0.48 ± 0.03
CLX3 (n = 4)	0.90 ± 0.01	0.87 ± 0.01	0.60 ± 0.03
CLX4 (n = 4)	0.88 ± 0.01	0.86 ± 0.01	0.60 ± 0.03
CLX5 (n = 4)	0.82 ± 0.01	0.80 ± 0.01	0.46 ± 0.02

4. Conclusions

This study has investigated the effect of blending speed and time on the flow and morphological characteristics of dry powder inhalation excipients consisting of coarse and fine lactose together with magnesium stearate. The results confirm the performance-enhancing capability of magnesium stearate, as consistent with earlier findings (Jetzer et al., 2018; Shur et al., 2016).). The improvement of coating with increasing blending speed from 500 rpm to 1500 rpm is consistent with the fact that shear forces during blending are necessary and advantageous for sufficient coating of magnesium stearate on the lactose carriers. The significantly less coating reported at blending speeds of 500 and 1000 rpm shows that insufficient shear results in low coating. Conversely, the increase of the fraction of particles less than 4.5 μm (Q4.5) at the highest blending speeds (2000 and 2500 rpm) shows that very high shear tends to promote the attrition of coarse lactose without substantial improvement in flow properties or enhanced coating of the lactose surface. The investigation of the effect of blending duration show that time appears to be a less determinant factor in changing the flow properties of the lactose excipients. With the blending time increased from 5 to 15 min, the blend properties do not change significantly. However, if the blending time is too short, optimal coating with magnesium stearate is compromised – as shown by the SIMS signal ratio of Mg^+/Lac-K^+ for a blending time of 5 min. For this study, blending longer than 10 min did not necessarily produce a significant improvement in the extent of coating. This is evidenced by the slight decrease in the SIMS signal ratio of Mg^+/Lac-K^+ between the blending time of 10 min and 15 min. Consequently, optimizing process settings for a complete formulation typically involves a careful balance of the benefits and drawbacks of blending speed and time, among other considerations. These results provide valuable insights for formulation scientists. While shear and time are essential for breaking and reforming inter-particle forces and bonds during mixing, the selection of optimal process settings must be approached holistically, considering the interplay among various process variables.

The results of water contact angles as an indicator of the extent of magnesium stearate coating is consistent with findings from earlier studies that show that higher water contact angles are indicators of better coating. Furthermore, the use of advanced imaging techniques like SEM and, particularly, ToF-SIMS also provides interesting insights to the extent of coating. It's worth noting that for ToF-SIMS, the selection of robust and reliable marker peaks and the interpretation of the data are of paramount importance. As shown, the sodium or potassium adduct of lactose provide reliable markers being advantageous over smaller fragments used in earlier studies.

As further work, the applicability of these findings to formulations containing active ingredients should be studied. Additionally, other important aspects like stability studies, filler selection, aerodynamic properties, fine particle fraction, etc. should be duly considered.

Table 5
SIMS signal ratios for I(Mg^+) / Σ (I(Mg^+), I(CH_3O^+)), respectively I(Mg^+) / Σ (I(Mg^+), I($C_2H_5O^+$)), and I(Mg^+) / Σ (I(Mg^+), I($C_3H_5O_2^+$)).

	CH_3O^+ basis	$C_2H_5O^+$ basis	$C_3H_5O_2^+$ basis
CLX-T1 (n = 4)	0.91 ± 0.05	0.88 ± 0.01	0.87 ± 0.02
CLX-T2 & CLX3 (n = 8)	0.90 ± 0.01	0.87 ± 0.01	0.84 ± 0.03
CLX-T3 (n = 4)	0.89 ± 0.01	0.88 ± 0.01	0.83 ± 0.04

Funding

This research did not receive any specific grant from funding agencies in the public, commercial, or not-for-profit sectors.

Declaration of Competing Interest

The authors declare that they have no known competing financial interests or personal relationships that could have appeared to influence the work reported in this paper.

Data availability

Data will be made available on request.

Acknowledgements

We thank Elke Sternberger-Rützel and Marco Laackmann for proof reading the manuscript. We thank Gerald Hebbink for support in scanning electron microscopy and Gerard Boswinkel for support in blending experiments.

References

Alghunaim, A., Kirdponpattara, S., Newby, B.M.Z., 2016. Techniques for determining contact angle and wettability of powders. Powder Technol. 287, 201–215.

Bolhuis, G.K., De Jong, S.W., Lerk, C.F., Dettmers, H., Pharbita, B.V., 1987. The effect of magnesium stearate admixing in different types of laboratory and industrial mixers on tablet crushing strength. Drug Dev. Ind. Pharm. 13 (9-11), 1547–1567.

Chander, S., Hogg, R., Fuerstenau, D.W., 2007. Characterization of the wetting and dewetting behavior of powders. Kona 25 (0), 56–75.

D. Cocconi M.D. Alberi A. Busca F. Schiaretti 2012. USE OF MAGNESIUM STEARATE IN DRY POWDER FORMULATIONS FOR INHALATION.

de Boer, A.H., Hagedoorn, P., Hoppentocht, M., Buttini, F., Grasmeijer, F., Frijlink, H.W., 2017. Dry powder inhalation: Past, present and future. Expert Opin Drug Del 14 (4), 499–512.

Depalo, A., Santomaso, A.C., 2013. Wetting dynamics and contact angles of powders studied through capillary rise experiments. Colloids and Surfaces a-Physicochemical and Engineering Aspects 436, 371–379.

Galet, L., Ouabbas, Y., Chamayou, A., Grosseau, P., Baron, M., Thomas, G., 2010a. Surface analysis of silica gel particles after mechanical dry coating with magnesium stearate. Kona Powder Part. J. 28 (0), 209–218.

Galet, L., Patry, S., Dodds, J., 2010b. Determination of the wettability of powders by the Washburn capillary rise method with bed preparation by a centrifugal packing technique. J. Colloid Interface Sci. 346 (2), 470–475.

M.M.J. Green K. Vale M. Perkins P. Whiteside 2009. Surface Coating of Lactose and API Particles with Magnesium Stearate, in: Dalby, R.N., Byron, P.R., Peart, J., Suman, J. D., Young, P.M. (Eds.), Respiratory Drug Delivery Europe 2009 445 448.

Guchardi, R., Frei, M., John, E., Kaerger, J., 2008. Influence of fine lactose and magnesium stearate on low dose dry powder inhaler formulations. Int. J. Pharm. 348 (1-2), 10–17.

Hebbink, G.A., Jaspers, M., Peters, H.J.W., Dickhoff, B.H.J., 2022. Recent developments in lactose blend formulations for carrier-based dry powder inhalation. Adv. Drug Deliv. Rev. 189, 114527.

Hertel, M., Schwarz, E., Kobler, M., Hauptstein, S., Steckel, H., Scherließ, R., 2018. Powder flow analysis: A simple method to indicate the ideal amount of lactose fines in dry powder inhaler formulations. Int. J. Pharm. 535 (1-2), 59–67.

Jetzer, M.W., Schneider, M., Morrical, B.D., Imanidis, G., 2018. Investigations on the mechanism of magnesium stearate to modify aerosol performance in dry powder inhaled formulations. J Pharm Sci-Us 107 (4), 984–998.

Kinnunen, H., Hebbink, G., Peters, H., Shur, J., Price, R., 2014. An investigation into the effect of fine lactose particles on the fluidization behaviour and aerosolization performance of carrier-based dry powder inhaler formulations. AAPS PharmSciTech 15 (4), 898–909.

Kinnunen, H., Hebbink, G., Peters, H., Huck, D., Makein, L., Price, R., 2015. Extrinsic lactose fines improve dry powder inhaler formulation performance of a cohesive batch of budesonide via agglomerate formation and consequential co-deposition. Int. J. Pharm. 478 (1), 53–59.

M.R. Mehta K. Pawar G.A. Hebbink H. Kinnunen J. Shur R. Price H. Peters 2018. Understanding the Influence of Device and Lactose Fines on Flow Properties and In Vitro Deposition from Dry Powder Inhalers, in: Dalby, R.N., Peart, J., Young, P.M., Traini, D. (Eds.), Respiratory Drug Delivery Asia 2018 193 198.

Mitchell, R., Marzolini, N.L., Hancock, S.A., Harridance, A.M., Elder, D.P., 2006. The use of surface analysis techniques to determine the route of manufacture of tablet dosage forms. Drug Dev. Ind. Pharm. 32 (2), 253–261.

Monteith, John, M., GlaxoSmithKline, Thoma, Marian, s., GlaxoSmithKline, 2004. Pharmaceutical Formulations Comprising Magnesium Stearate. Glaxo Group Limited.

Peddapatla, R.V.G., Ahmed, M.R., Blackshields, C.A., Sousa-Gallagher, M.J., McSweeney, S., Kruse, J., Crean, A.M., Fitzpatrick, D., 2018. Broadband acoustic resonance dissolution spectroscopy (BARDS): A novel approach to investigate the wettability of pharmaceutical powder blends. Mol Pharmaceut 15 (1), 31–39.

Qu, L.i., Zhou, Q., Gengenbach, T., Denman, J.A., Stewart, P.J., Hapgood, K.P., Gamlen, M., Morton, D.A.V., 2015. Investigation of the potential for direct compaction of a fine ibuprofen powder dry-coated with magnesium stearate. Drug Dev. Ind. Pharm. 41 (5), 825–837.

Rahmanian, N., Ng, B., Hassanpour, A., Ding, Y., Antony, J., Jia, X., Ghadiri, M., van der Wel, P., Krug-Polman, A., York, D., Bayly, A., Tan, H.S., 2008. Scale-up of high-shear mixer granulators. Kona Powder Part. J. 26 (0), 190–204.

Shur, J., Harris, H., Jones, M.D., Kaerger, J.S., Price, R., 2008. The role of fines in the modification of the fluidization and dispersion mechanism within dry powder inhaler formulations. Pharm. Res. 25 (7), 1631–1640.

Shur, J., Price, R., Lewis, D., Young, P.M., Woollam, G., Singh, D., Edge, S., 2016. From single excipients to dual excipient platforms in dry powder inhaler products. Int. J. Pharm. 514 (2), 374–383.

Sun, Y., Yu, D., Li, J.Y., Zhao, J.A., Feng, Y., Zhang, X., Mao, S.R., 2022. Elucidation of lactose fine size and drug shape on rheological properties and aerodynamic behavior of dry powders for inhalation. Eur. J. Pharm. Biopharm. 179, 47–57.

Teipel, U., Mikonsaari, I., 2004. Determining contact angles of powders by liquid penetration. Part. Part. Syst. Char. 21 (4), 255–260.

United States Pharmacopeia , 2013 . Bulk density and tapped density of powders. Rockville, MD, pp. 265 – 268.

Wang, Z., Chu, Y., Zhao, G., Yin, Z., Kuang, T., Yan, F., Zhang, L., Zhang, L.u., 2023. Study of surface wettability of mineral rock particles by an improved washburn method. ACS Omega 8 (17), 15721–15729.

Weiss, C., McLoughlin, P., Cathcart, H., 2015. Characterisation of dry powder inhaler formulations using atomic force microscopy. Int. J. Pharm. 494 (1), 393–407.

Zhou, Q., Qu, L.i., Gengenbach, T., Denman, J.A., Larson, I., Stewart, P.J., Morton, D.A. V., 2011. Investigation of the extent of surface coating via mechanofusion with varying additive levels and the influences on bulk powder flow properties. Int. J. Pharm. 413 (1-2), 36–43.